

Universal light quark mass dependence and heavy-light meson spectroscopy

Theodore J. Allen

*Department of Physics, Hobart & William Smith Colleges,
Geneva, NY 14456 USA*

Todd Coleman

*Joint Science Department, Claremont McKenna,
Pitzer, and Scripps Colleges,
925 N. Mills Ave., Claremont, CA 91711 USA*

M.G. Olsson

*Department of Physics, University of Wisconsin,
1150 University Avenue, Madison, WI 53706 USA*

Siniša Veseli

*Fermi National Accelerator Laboratory,
P.O. Box 500, Batavia, IL 60510 USA*

Clean predictions are presented for all the spin-averaged heavy-light meson spectroscopies. A new symmetry is identified wherein the energy eigenstates have a universal dependence on both the light and heavy quark masses. This universality is used in an efficient analysis of these mesons within the QCD string/flux tube picture. Unique predictions for all the D , D_s , B , and B_s type mesons in terms of just four measured quantities.

I. INTRODUCTION

One of the most promising and least developed areas of hadron spectroscopy is the excited heavy-light (HL) meson. Although at present only a few states of each flavor have been observed future discoveries at B factories, CLEOc, HERA, and hadron colliders will surely change this situation. In addition to the ordinary $q\bar{Q}$ states we should observe hybrid and possibly multi-quark confined mesons. It is important therefore to reliably predict where the standard HL mesons lie and to explore the close relationship between the D , D_s , B and B_s families of HL mesons.

A striking observed fact for HL systems is that hyperfine splittings are independent of light quark flavor. For example [1]

$$D_s^* - D_s \simeq D^* - D \simeq 142 \text{ MeV}, \quad (1)$$

$$B_s^* - B_s \simeq B^* - B \simeq 46 \text{ MeV}. \quad (2)$$

This apparent lack of light quark mass dependence in these differences is certainly not that expected in the popular Breit-Fermi type semi-relativistic interaction which is proportional to the inverse product of the quark masses ($1/m_Q m$). In the following we show that this is an example of a larger “universal light quark mass dependence” (UMD) ultimately a consequence of relativistic kinematics. We note in passing that the ratio of the above hyperfine differences does however reflect the inverse ratio of the heavy quark masses.

We start by proposing and supporting the concept that all HL energy eigenstates have the same light quark mass dependence and hence all differences containing the same light flavor are independent of light quark mass. We take

this as an organizing principle to analyze the various HL systems. In particular we find a functional relation between strange and non-strange light quark masses, m_s and $m_{u,d}$, and we predict the spectra for the D , D_s , B , and B_s systems. In Sec. II we establish the UMD principle first from experiment, then from a model calculation. We finally exhibit the UMD within a simple potential model. In Sec. III we use UMD to determine the parameters of the relativistic flux tube, a simple but fundamental model. These parameters are the Coulomb constant and the heavy quark masses m_c and m_b . Another application of UMD is given in Sec. IV where from the measured difference $B_s - B$, a relationship between the constituent quark masses m_s and $m_{u,d}$ is established. This relationship is also shown to follow from relativistic kinematics alone. In Sec. V we use our results to predict a range of radially and orbitally excited HL mesons.

II. UNIVERSAL LIGHT QUARK MASS DEPENDENCE

The HL meson mass M , in the heavy quark limit, can be defined in terms of the excitation energy E and the heavy quark mass m_Q as

$$M = m_Q + E. \quad (3)$$

As we will demonstrate, the meson mass M has universal mass dependence on both the heavy quark mass m_Q and the light quark mass m . Up to $1/m_Q$ corrections, we may expand E as

$$E_{n,\ell} = E_{n,\ell}(0) + \beta m^2 + \dots, \quad (4)$$

where the coefficient β is independent of both the radial number n and the angular quantum number ℓ . We expect the expansion to have only even powers of m since m only appears quadratically in our model Hamiltonians. The energy differences between different HL excitations is then

$$E_2 - E_1 = E_2(0) - E_1(0) + \beta(m_2^2 - m_1^2) + \dots \quad (5)$$

The excitation energy differences of HL mesons with the same light flavor are independent of the quark mass. We offer three types of evidence for this (UMD) universality.

A. Experimental Data

We select any convenient P -wave and S -wave D type meson difference [1]. For example,

$$D_1(2422 \pm 2 \text{ MeV}) - D(1864 \pm 0.5 \text{ MeV}) = 558 \pm 2 \text{ MeV}. \quad (6)$$

We now compare this with the corresponding D_s difference,

$$D_{s1}(2535 \pm 0.5 \text{ MeV}) - D_s(1969 \pm 1.4 \text{ MeV}) = 566 \pm 1.5 \text{ MeV}. \quad (7)$$

If UMD is valid, the two differences should be identical. Experimentally they differ by $8 \pm 3 \text{ MeV}$ which is an accuracy of better than 2%.

Other differences involving D^* and D_2 give similar results but with slightly larger errors.

B. A dynamical model: the relativistic flux tube

The Relativistic Flux Tube (RFT) (or QCD string) model with spinless quarks has been solved numerically for about a decade [2]. For a rigorous derivation and experimental motivation see [3]. We will not discuss the details of this model here except to emphasize that it is a very realistic model incorporating many of the features of QCD. In addition to the string confinement (with static tension a) we add a short range interaction $U(r) = -k/r$. In the heavy quark limit the heavy quark mass appears additively as in Eq. (3) with no $1/m_Q$ corrections. The light quark constituent mass is not well known and we will only assume that it is in the range $0 < m < 600 \text{ MeV}$. The parameters that appear in the RFT model are the string tension a , the Coulomb constant k , and the masses of the heavy quark, m_Q , and the light quark, m . Since the quarks are spinless in this model we will always compare our model predictions to the spin-averaged data.

In this sub-section we are exploring the properties of the RFT model and not comparing to experimental data so the exact values of the parameters are not important. We use $a = 0.18 \text{ GeV}^2$ and $k = 0.5$ which are in fact reasonable values, as we discuss in the next section. In Fig. 1 we plot the lowest S and P wave eigenvalues of the excitation energy E as a function of the light quark mass m . The

important thing to notice is that the difference $1P - 1S$ is quite constant. This is exactly what is expected under UMD as in Eqs. (4) or (5).

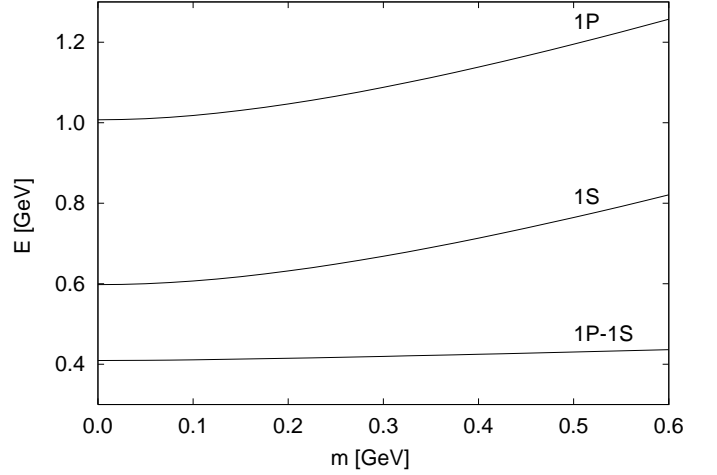


FIG. 1: Light quark mass dependence of the lowest S and P -wave heavy-light excitation energies as predicted by the relativistic flux tube model. We note that the $1P - 1S$ mass difference is nearly independent of light quark mass.

C. A simple analytic result

We show here that UMD is fundamentally a result of relativistic kinematics. Let us consider a simple time-component vector potential model with relativistic kinematics,

$$H\psi = E\psi, \quad (8)$$

$$H = \sqrt{\mathbf{p}^2 + m^2} + U(r), \quad (9)$$

where

$$\mathbf{p}^2 = p_r^2 + L^2/r^2. \quad (10)$$

An expression of UMD is

$$\partial^2 E / \partial L^2 \partial m^2 = 0. \quad (11)$$

We can demonstrate this to leading order with the Feynman-Hellmann theorem [4]

$$\partial E / \partial \lambda = \langle \partial H / \partial \lambda \rangle, \quad (12)$$

where λ is a system parameter. The desired quantity (11) is then given by

$$\partial^2 E / \partial L^2 \partial m^2 = \langle \partial^2 H / \partial L^2 \partial m^2 \rangle. \quad (13)$$

Expanding about $L^2 = m^2 = 0$ we find from (9) that

$$H = p_r + (L^2/r^2 + m^2)/(2p_r) + \dots \quad (14)$$

which then yields to leading order

$$\partial^2 E / \partial L^2 \partial m^2 = 0. \quad (15)$$

The above demonstration of light quark universality also holds for mesons with two light quark mesons.

The next term in the expansion (14) is a cross term proportional to $L^2 m^2$, which yields a non-vanishing second derivative (15) that violates UMD. A similar violation using the RFT model can be seen in Fig. 1 and amounts to about 10 MeV for m increasing from 300 MeV to 500 MeV. This accounts for the small observed violation of 8 ± 3 MeV noted in Eqs. (6) and (7).

III. THE RFT PARAMETERS a , k , m_c , m_b

As we have noted the parameters entering the RFT model are the string tension a , the Coulomb constant k , and the two heavy quark masses m_c and m_b . The predictions for excited states will be nearly independent of the light quark mass value but sensitive to the difference between m_s and $m_{u,d}$.

A. String tension

The universal Regge slope for both mesons and baryons is [5],

$$\alpha' = 0.88 \text{ GeV}^2 \quad (16)$$

For a relativistically rotating QCD string, the Nambu-Goto QCD string [6] and the RFT model predict the Regge slope to be

$$\alpha' = 1/2\pi a, \quad (17)$$

which yields the string tension,

$$a = 0.18 \text{ GeV}^2. \quad (18)$$

This value is quite consistent with that obtained from an analysis of heavy onia data alone [7] and we will assume it in our subsequent work.

B. Coulomb constant

Without any assumptions about the quark masses, we can find the Coulomb constant using UMD as an organizing principle. The idea is to compare the model predictions with an experimental $1P - 1S$ HL mass difference. To do this we must know the masses of a pair of spin averaged states. Fortunately, we now have a complete set of states for the D_s mesons due to recent B factory measurements [8] and older data [1]. We find the spin averaged (weighted

by angular momentum multiplicity) states to be

$$D_{s,1S} = \frac{3}{4}D_s^* + \frac{1}{4}D_s = 2076 \pm 1 \text{ MeV}, \quad (19)$$

$$\begin{aligned} D_{s,1P} &= \frac{1}{12}D_{s,0+} + \frac{1}{4}(D_{s,1+}^{1/2} + D_{s,1+}^{3/2}) + \frac{5}{12}D_{s,2+} \\ &= 2515 \pm 3 \text{ MeV}. \end{aligned} \quad (20)$$

We need the difference

$$D_{s,1P} - D_{s,1S} = 439 \pm 4 \text{ MeV}. \quad (21)$$

In Fig. 2 we show the RFT prediction for this difference as a function of the Coulomb constant k and we see that the correct value is,

$$k \simeq 0.52. \quad (22)$$

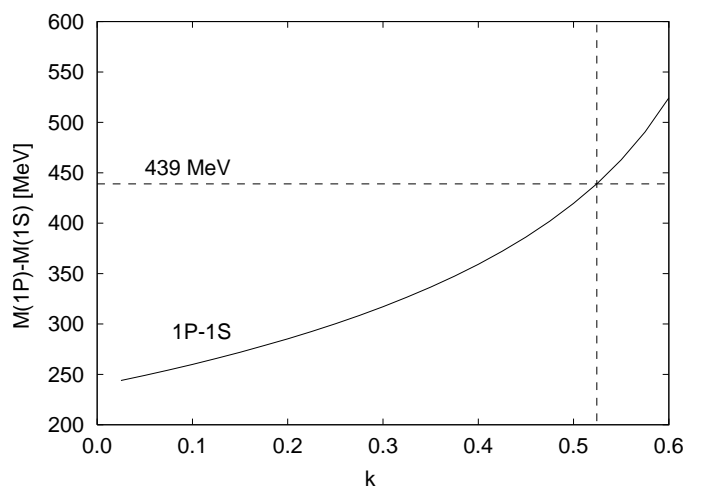


FIG. 2: The difference of the lowest S and P wave heavy-light meson masses in the RFT model as a function of the Coulomb constant k . The horizontal line is the experimental value (21) determined from the D_s states.

C. Heavy quark masses

The heavy quark masses do depend on the choice of light quark mass. In order to agree with the observed $1S$ state we must adjust m_Q as m is varied. The results for the charm and bottom quarks are shown in Figs. 3 and 4.

IV. RELATION BETWEEN THE LIGHT QUARK MASSES

For a given heavy quark, say the b , the two ground state mesons B_s and B are expected to differ in mass as given in Eq. (5) since β is not zero. Experimentally this difference is [1]

$$B_s - B = 91 \pm 1 \text{ MeV}. \quad (23)$$

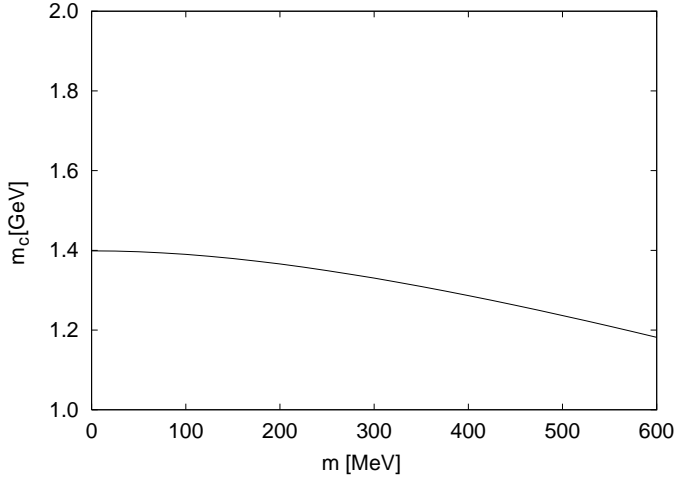


FIG. 3: The c quark mass required to yield the observed spin averaged D_{1S} meson mass for a range of choices of light quark mass.

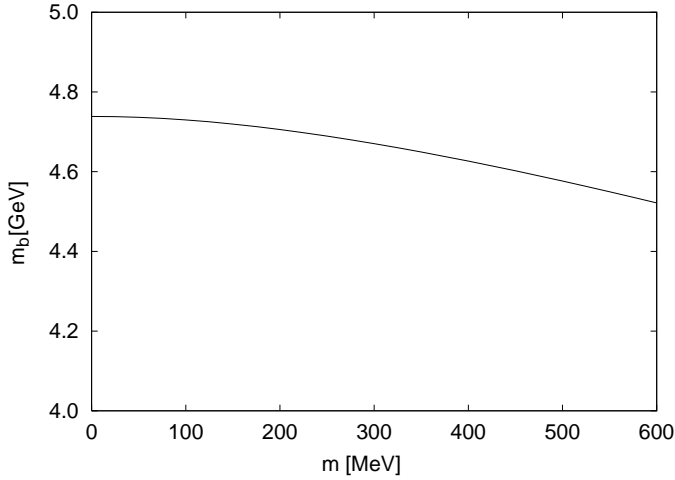


FIG. 4: The b quark mass required to yield the observed spin averaged B_{1S} meson mass for a range of choices of light quark mass.

This observation implies a functional relation between the strange and non-strange quark masses. Using the values for a and k in Eqs. (18) and (22), we exhibit this relation for the RFT model in Fig. 5. We might note that the corresponding charm difference is about 10 MeV larger and reflects a larger heavy quark kinetic energy (*i.e.*, a $1/m_Q$ correction). Finally, we might comment that this relation between quark masses again arises primarily from relativistic kinematics. The relation

$$\sqrt{p_0^2 + m_s^2} - \sqrt{p_0^2 + m_{u,d}^2} = 91 \text{ MeV} \quad (24)$$

follows from the simple Hamiltonian (9). With the choice $p_0^2 = 0.4 \text{ GeV}^2$ as the average square momentum, the implicit relationship of Eq. (24) parallels that of the more realistic RFT nicely and is depicted on Fig. 5 by the dashed curve. We also include the solutions for the light quark

constituent masses obtained from analyses of hyperon magnetic moments. We note that these “hyperon” values of the light quark masses fall close to our curve.

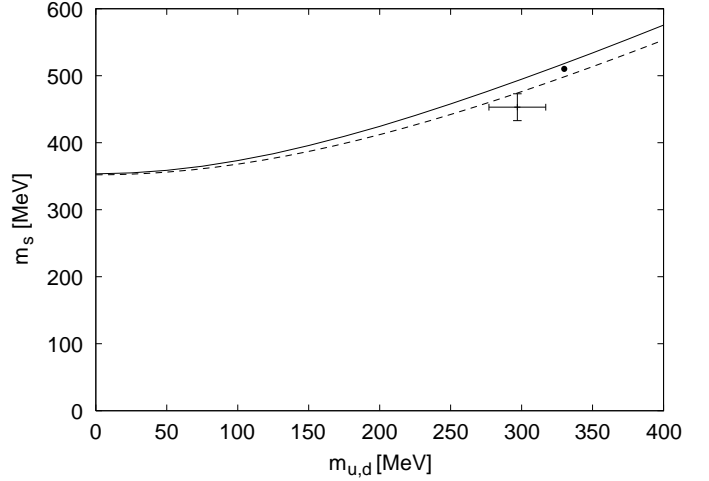


FIG. 5: The relation between the strange and the non-strange light quark masses required to maintain the relation (23). The “data” points corresponds to the well known and successful hyperon magnetic moment model where the quarks have Dirac moments inversely proportional to the constituent quark masses [1] (dot) and [9] (error bar). The solid curve is the prediction of the relativistic flux-tube (RFT) model. The dashed curve is computed using the pure relativistic kinematics of Eq. (24) with $p_0^2 = 0.4 \text{ GeV}^2$.

V. PREDICTIONS FOR THE HEAVY-LIGHT SPECTRA

Now that the parameters of the RFT model have been fixed, we can make a range of predictions. We note that we have required only the S -wave spin averaged ground states for the charm and bottom states, and one spin averaged P -wave multiplet (in our case the D_s). The predictions are then unique and independent of specific choices of the light quark masses. In Figs. 6 to 9 we present our predictions for the D , D_s , B , and B_s flavor families. In each case we predict up to five radial and five angular states. As we expect from UMD, the predictions are nearly unique. If the light quark mass is varied over a 200 MeV range, the predictions for the excited states vary by less than 10 MeV, which would be difficult to see on the figures. In Table 1 we provide the numerical predictions for the spin-averaged states assuming $m_{u,d} = 300 \text{ MeV}$ and $m_s = 500 \text{ MeV}$.

VI. CONCLUSIONS

We have approached the subject of heavy-light meson spectroscopy by introducing a new principle which we call “universal light quark mass dependence” (UMD). The idea is that the energies of all orbitally and radially excited

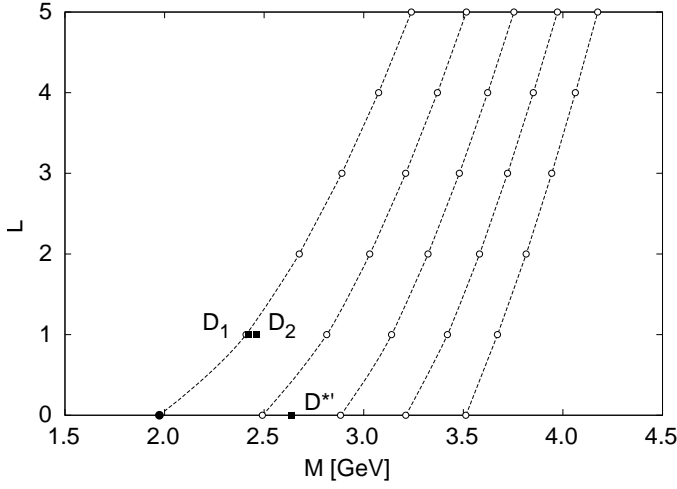


FIG. 6: The $D(cu, cd)$ spectroscopy. The large solid dot is input data and the hollow dots are predicted states. The predicted states are displayed numerically in Table 1. The boxes represent measured (spin) states not used in the calculation. The $D_1(2420)$ and $D_2(2460)$ are well known but the $D^*(2637)$ [10] should be verified.

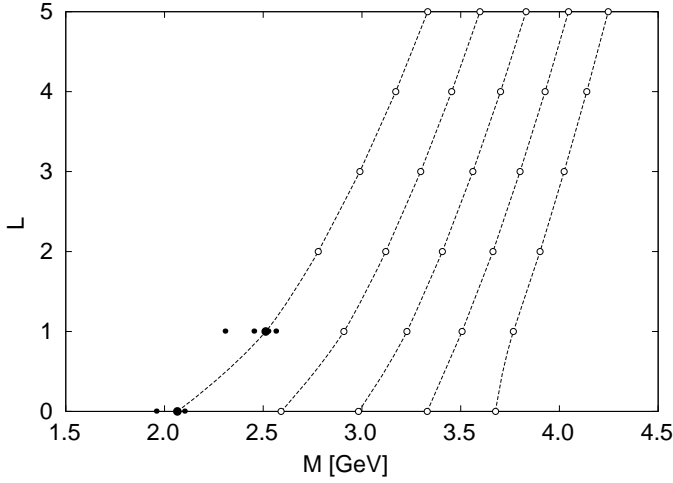


FIG. 7: The $D_s(cs)$ spectroscopy. The large solid dots are input data and the hollow dots are predicted states. The predicted states are displayed numerically in Table 1. To illustrate the spin dependence we show the 1S and 1P spin states as small dots.

states vary in the same way as the light quark mass is varied. This proposal is supported in Sec. II by experimental evidence, numerical calculations using a realistic theoretical model, and finally by analytic demonstration using a simple but relativistic potential model. This universality observation makes the analysis of heavy-light mesons transparent and considerably simpler. We further note that the measured $B_s - B$ difference implies a functional relation between the strange and non-strange light quark masses which is consistent with the well known quark model of the hyperon magnetic moments [1, 9]. From only the S -wave states and one spin-averaged P -wave state, the

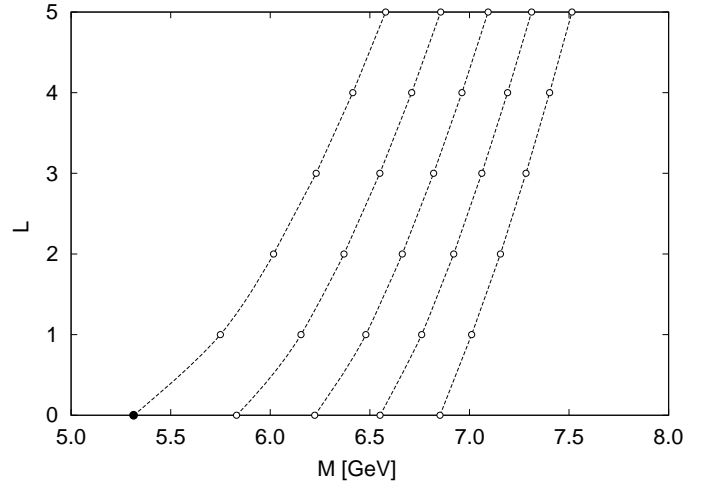


FIG. 8: The $B(bu, bd)$ spectroscopy. The solid dot is input data and the hollow dots are predicted states. The predicted states are displayed numerically in Table 1.

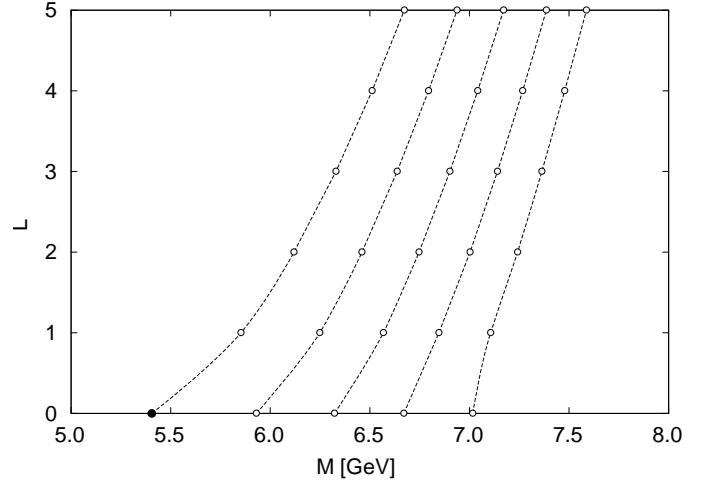


FIG. 9: The $B_s(bs)$ spectroscopy. The solid dot is input data and the hollow dots are predicted states. The predicted states are displayed numerically in Table 1.

D_s , we can reliably predict the D , D_s , B , and B_s excited spectrum. It should be noted that our predictions are for the spin-averaged states and that we assumed that the heavy-light assumption is valid. There are some small discrepancies in the data when thought of in the heavy-light limit. For example $D_s - D$ is about 10 percent larger (10 MeV) than the corresponding difference $B_s - B$. This is probably due to $1/m_Q$ corrections to heavy quark symmetry. Another topic for future investigation is the breakdown of the heavy-light approximation for highly excited states.

TABLE I: Predicted heavy-light meson states in GeV. The flux tube parameters are $a = 0.18 \text{ GeV}^{-2}$, $k = 0.524$, $m_{u,d} = 300 \text{ MeV}$, $m_s = 495 \text{ MeV}$, $m_c = 1330 \text{ MeV}$, $m_b = 4670 \text{ MeV}$. These states are illustrated in Figs. 6–9. Varying the light quark masses over a range of 200 MeV changes our predictions by less than 10 MeV.

	n			
	1	2	3	4
ℓ	D states			
0	1.974	2.491	2.883	3.211
1	2.409	2.814	3.140	3.420
2	2.677	3.030	3.323	3.581
3	2.891	3.210	3.480	3.722
	D_s states			
0	2.065	2.590	2.982	3.331
1	2.513	2.909	3.228	3.507
2	2.779	3.120	3.407	3.663
3	2.990	3.297	3.562	3.801
	B states			
0	5.314	5.831	6.223	6.551
1	5.749	6.154	6.480	6.760
2	6.017	6.370	6.663	6.921
3	6.231	6.550	6.820	7.062
	B_s states			
0	5.405	5.930	6.322	6.671
1	5.853	6.249	6.568	6.847
2	6.119	6.460	6.747	7.003
3	6.330	6.637	6.902	7.141

Acknowledgment

This work was supported in part by the US Department of Energy under Contract No. DE-FG02-95ER40896.

-
- [1] K. Hagiwara, *et al.*, Phys. Rev. D **66**, 010001 (2002).
 - [2] D. La Course and M. G. Olsson, Phys. Rev. D **39**, 2751 (1989); M. G. Olsson and S. Veseli, Phys. Rev. D **51**, 3578 (1995); C. Semay and B. Silvestre-Brac, Phys. Rev. D **52**, 6553 (1995).
 - [3] T. J. Allen and M. G. Olsson, Phys. Rev. D **68**, 032002 (2003) [hep-ph/0306128].
 - [4] H. Hellmann, *Einführung in die Quantenchemie*, (Deuticke Verlag, Leipzig, 1937); R.P. Feynman, Phys. Rev. **56**, 340 (1939).
 - [5] V. Barger and D. Cline, *Phenomenological Theories of High Energy Scattering: An Experimental Evaluation*, (W. A. Benjamin, New York, 1969).
 - [6] Y. Nambu, “Quark model and the factorization of the Veneziano Amplitude,” in *Symmetries and quark models*, edited by R. Chand, (Gordon and Breach, New York, 1970); T. Goto, Prog. Theor. Phys. **46**, 1560 (1971); L. Susskind, Nuovo Cimento **69A**, 457 (1970); A. M. Polyakov, Phys. Lett. B **103**, 207 (1981); B. M. Barbashov and V. V. Nesterenko, *Introduction to the Relativistic String Theory*, (World Scientific, Singapore, 1990).
 - [7] Steve Jacobs, M.G. Olsson, and Casimir Suchyta III, Phys. Rev. D **33**, 3338 (1986).
 - [8] The narrow P -wave $D_s(2460)$ and $D_s(2317)$ have recently been observed at the CLEO (D. Besson, *et al.*, Phys. Rev. D **68**, 032002 (2003) [hep-ex/0305100]), BABAR, and Belle detectors.
 - [9] Jerrold Franklin, Phys. Rev. D **66** 033010 (2002) .
 - [10] P. Abreu, *et al.* (DELPHI Collaboration), Phys. Lett. B **426**, 231 (1998).